

AN EFFICIENT HAAR WAVELET SERIES METHOD TO SOLVE HIGHER-ORDER MULTI-PANTOGRAPH EQUATIONS ARISING IN ELECTRODYNAMICS

AFROZ⁽¹⁾, BASHARAT HUSSAIN⁽²⁾ AND ABDULLAH⁽³⁾

ABSTRACT. The primary aim of this paper is to develop a numerical method based on Haar wavelets for solving second and higher-order multi-pantograph differential equations. This method transforms the differential equation into a system of algebraic equations with undetermined coefficients. These algebraic systems can be solved either by Newton's or Broyden's iterative methods. Finally, few test examples are taken from the literature to show the computational efficiency of this method.

1. INTRODUCTION

Delay differential equations appeared in the mathematical modeling of many real-world processes. It has enormous applications in many fields such as probability theory, number theory, chemical, and biological processes, population and economic growth modeling, etc. Functional-differential equation with proportional delay is known as pantograph equation or generalized pantograph equation. The name pantograph first appeared in 1851 and was a device used in the construction of the electric locomotive. The mathematical model of pantograph was first developed by Ockendon and Tyler [19]. Pantograph equation is one of the most distinguished delay differential equation and has been an interest of many researchers [5, 9, 10]. The pantograph differential equations are encountered in studies of population dynamic model, quantum theory, control theory, cell growth model, disease spread model and

2010 *Mathematics Subject Classification.* 34Kxx , 65L03, 65L05 ,65L60.

Key words and phrases. Pantograph equations; Delay Ordinary Differential Equation; Numerical method; Collocation points; Haar wavelets.

Copyright © Deanship of Research and Graduate Studies, Yarmouk University, Irbid, Jordan.

Received: March 23 ,2021

Accepted: July 14, 2021 .

astrophysics [9]. These equations also have several industrial applications and play a central role in the mathematical modeling of train's overhead current collection system [19]. The continuous electricity supply between the catenary and the train's motor is maintained by a device called a z -shape pantograph. The z -shape pantograph (also known as half pantograph) resembled the pantograph device for copying, writing, and drawing. It has a spring mechanism to push the contact shoe against the wire to draw the electricity needed to run the train.

Most of these equations can not be solvable exactly. Therefore, a numerical technique is required to obtain their approximate solutions. Variational iteration method [8], one leg- θ method [26], two-stage R-K method [28], reproducing kernel Hilbert space method (RKHSM) [15], differential transform method [12], adomain decomposition method [6], perturbed iteration method [4] are some already established numerical techniques to solve such types of differential equations. Recently, in [3] Time-invariant and time-varying first-order delay differential equations have been solved using the Haar wavelet collocation method. Some other collocation methods are also developed using Chebyshev Polynomials, Hermite Polynomials, Bernoulli Polynomials for detail reader may refer to [14, 24, 29] respectively.

Chen-Hsiao [7] gave an idea of utilizing Haar operational matrix of integration for solving differential equations. In the existing literature, the development and application of the Haar wavelet collocation method (HWCM) for solving differential equations are based on the method given by Chen and Hsiao. Later this idea has been extended for solving a wide range of problems[13]. Marzban and Razzaghi [18] adapted the rationalized Haar wavelet approach for solving nonlinear optimal control problem. Haar wavelet collocation method is also a valuable tool in structural mechanics, Hariharan [11] applied the Haar wavelet-based technique for solving finite length beam equation. Lepik [13] discussed buckling of elastic beams using the Haar wavelet method. In [20] Patra and Saha obtained the solution of stiff point kinetics equations using wavelet operational method based on Haar wavelet. In the recent past the Chen-Hsiao's technique is extended to solve delay differential equations, Aziz and Amin[3] investigated the approximate solution of delay differential as well as partial delay differential equations. Raza et al. [21] transform the delay

term using Taylor series expansion and then applied the Haar wavelet collocation method to solve singularly perturbed differential-difference equations and singularly perturbed convection delayed dominated diffusion equations. Abdullah and Rafiq [1] combined the backward Euler method and Haar wavelet collocation method to obtain the approximate solution of the Chen-Lee-Liu equation.

Haar wavelets consist of pairs of piece-wise constant functions and are not differentiable. Unlike Daubechies, Coiflet, Symlet, Haar wavelets are the simplest wavelets that have an analytic mathematical expression. The solution obtained using Haar wavelets are usually simpler, faster, and computationally attractive.

In [17, 16] Majak et al. discuss the convergence analysis and accuracy issues of Chen-Hasio's approach based Haar wavelet collocation method. It is pointed out in [17] that the order of convergence equals two. In [17] authors have proved the following convergence theorem:

Theorem 1.1. *Let us assume that $u(t) = \frac{\partial^n \omega(t)}{\partial t^n}$ be square integrable function with bounded first derivative on $[0, 1]$, then the Haar wavelet collocation method will be convergent i.e. $\|E_M\|_2$ (L^2 - norm of error function) vanishes as J goes to infinity. Also, the convergence is of order two*

$$\|E_M\|_2 = O \left[\left(\frac{1}{2^{J+1}} \right)^2 \right].$$

In the present study, we have applied a modified Haar wavelet series method (MHWSM) instead of the conventional Haar wavelet collocation method. Here we have expanded the $(n + 1)^{th}$ order derivative involves in the differential equations in terms of Haar series instead of the n^{th} (highest) order derivative. The MHWSM produced a smoother solution than the Haar wavelet collocation method, therefore a significant decrease in absolute error is expected. The rest of this manuscript is organized as follows. In section 2, we briefly discuss the definition of the Haar wavelet family and their integrals. Section 3 deals with the development of the Modified Haar wavelet series method (MHWSM). Section 4 deals with the algorithm of the scheme. Brief convergence analysis of the Haar wavelet is provided in Section 5. In Section 6, several illustrative examples are given to test the ability, accuracy, and convergence of the method.

2. HAAR WAVELET

The Haar wavelet family on the interval $[0, 1)$ is defined as follows:

$$(2.1) \quad \mathbf{h}_i(t) = \begin{cases} 1 & \text{for } t \in [t_1(i), t_2(i)) \\ -1 & \text{for } t \in [t_2(i), t_3(i)) \\ 0 & \text{otherwise,} \end{cases}$$

where

$$t_1(i) = \frac{k}{m}, \quad t_2(i) = \frac{k+0.5}{m}, \quad t_3(i) = \frac{k+1}{m}.$$

Here $m = 2^j, j = 0, 1, \dots, J$ and $k = 0, 1, \dots, m-1$ is the translation parameter and J is the maximum level of resolution. The wavelet number i is given by $i = m + k + 1$, for $i \geq 2$. For $i = 1$, the function $\mathbf{h}_1(t)$ is father wavelet or scaling function for the family of Haar wavelet which is defined as follows:

$$\mathbf{h}_1(t) = \chi_{[0,1)}(t),$$

where $\chi_{[0,1)}(t)$ is characteristics function. For more detailed information about Haar wavelets, we refer to [2, 13, 22].

Any L^2 -space function defined on $[0, 1]$ can be approximated as the finite sum of Haar wavelet series as follows:

$$f(t) = \sum_{i=1}^{2M} a_i \mathbf{h}_i(t).$$

In the subsequent section we need the following integrals of Haar wavelets

$$I_\nu \mathbf{h}_i(t) = \int_0^t \int_0^t \int_0^t \cdots \int_0^t \mathbf{h}_i(z) d^\nu z = \frac{1}{(\nu-1)!} \int_0^t (t-z)^{\nu-1} \mathbf{h}_i(z) dz,$$

where $\nu = 1, 2, \dots, n$ and $i = 1, 2, \dots, 2^{J+1}$. Integration of (2.1) is carried out analytically to obtain these integrals and are given below:

$$(2.2) \quad I_n \mathbf{h}_i(t) = \frac{1}{n!} \begin{cases} 0 & \text{when } t \in [0, t_1(i)) \\ (t - t_1(i))^n & \text{when } t \in [t_1(i), t_2(i)) \\ (t - t_1(i))^n - 2(t - t_2(i))^n & \text{when } t \in [t_2(i), t_3(i)) \\ (t - t_1(i))^n - 2(t - t_2(i))^n + (t - t_3(i))^n & \text{when } t \in [t_3(i), 1). \end{cases}$$

3. NUMERICAL METHOD

Let us assume a n^{th} order pantograph equation of the form

$$\omega^n(t) = \varphi(g(t), \omega(\rho_0 t), \omega^1(\rho_1 t), \omega^2(\rho_2 t) \dots \omega^n(\rho_n t)), \forall t \in [t_0, t_f] \tag{3.1}$$

$$\text{with } \omega^\eta(0) = \omega_0^\eta,$$

where $\varphi : [t_0, t_f] \times \underbrace{R \times R \dots \times R}_{(n+1)\text{-times}} \mapsto R$ is a differentiable function, $g(t)$ is continuous on $[t_0, t_f]$ and $\rho_0, \rho_1 \dots \rho_n$ are real constants lies in $(0, 1]$. Also, $\omega^1, \omega^2 \dots \omega^n$ denotes the first, second and n^{th} order derivatives, respectively and ω_0^η are initial value conditions $\eta = 0, 1, 2 \dots n - 1$. Put $t = 0$ in 3.1 for $\omega^n(0)$.

In order to solve (3.1) we have established the following algorithm using Haar wavelet series. Let us suppose $\omega^{n+1}(t)$ be square integrable function. Therefore, we can write

$$\omega^{n+1}(t) = \sum_{i=1}^{2M} a_i \mathbf{h}_i(t). \tag{3.2}$$

Integrating (3.2) r ($r = 1, 2, \dots, n + 1$) times with respect to t , we have the following relation

$$\omega^{n+1-r}(t) = \sum_{i=1}^{2M} a_i I_r \mathbf{h}_i(t) + \sum_{\eta=n+1-r}^n \frac{\omega^\eta(0)(t)^{\eta-(n+1-r)}}{(\eta - (n + 1 - r))!}. \tag{3.3}$$

Taking $r = n + 1$ in relation (3.3), we have $\omega(t)$ as:

$$\omega(t) = \sum_{i=1}^{2M} a_i I_{n+1} \mathbf{h}_i(t) + \sum_{\eta=0}^n \frac{\omega^\eta(0)(t)^\eta}{(\eta)!}. \tag{3.4}$$

Also,

$$\omega(\rho_0 t) = \sum_{i=1}^{2M} a_i I_{n+1} \mathbf{h}_i(\rho_0 t) + \sum_{\eta=0}^n \frac{\omega^\eta(0)(\rho_0 t)^\eta}{(\eta)!}. \tag{3.5}$$

Similarly,

$$\omega^1(\rho_1 t) = \sum_{i=1}^{2M} a_i I_n \mathbf{h}_i(\rho_1 t) + \sum_{\eta=1}^n \frac{\omega^\eta(0)(\rho_1 t)^{\eta-1}}{(\eta - 1)!} \tag{3.6}$$

⋮

$$\omega^n(\rho_n t) = \sum_{i=1}^{2M} a_i I_1 \mathbf{h}_i(\rho_n t) + \omega^n(0). \tag{3.7}$$

Now, Substituting Eqs. (3.3 - 3.7) in Eq. (3.1), we get

$$(3.8) \quad \sum_{i=1}^{2M} a_i I_1 \mathbf{h}_i(t) + \omega^n(0) = \varphi \left(g(t), \sum_{i=1}^{2M} a_i I_{n+1} \mathbf{h}_i(\rho_0 t) + \sum_{\eta=0}^n \frac{\omega^\eta(0)(\rho_0 t)^\eta}{(\eta)!}, \right. \\ \left. \sum_{i=1}^{2M} a_i I_n \mathbf{h}_i(\rho_1 t) + \sum_{\eta=1}^n \frac{\omega^\eta(0)(\rho_1 t)^{\eta-1}}{(\eta-1)!}, \dots, \sum_{i=1}^{2M} a_i I_1 \mathbf{h}_i(\rho_n t) + \omega^n(0) \right)$$

Moreover, utilizing collocation points $t_l, l = 1, 2, \dots, 2M$ in Eq. (3.8), we obtain:

$$(3.9) \quad \sum_{i=1}^{2M} a_i I_1 \mathbf{h}_i(t_l) + \omega^n(0) = \varphi \left[g(t_l), \sum_{i=1}^{2M} a_i I_{n+1} \mathbf{h}_i(\rho_0 t_l) + \sum_{\eta=0}^n \frac{\omega^\eta(0)(\rho_0 t_l)^\eta}{(\eta)!}, \right. \\ \left. \sum_{i=1}^{2M} a_i I_n \mathbf{h}_i(\rho_1 t_l) + \sum_{\eta=1}^n \frac{\omega^\eta(0)(\rho_1 t_l)^{\eta-1}}{(\eta-1)!}, \dots, \sum_{i=1}^{2M} a_i I_1 \mathbf{h}_i(\rho_n t_l) + \omega^n(0) \right]$$

Now, we can easily find the coefficients a_i 's using any iterative techniques like Newton's method or Broyden's method. Finally, the solution is obtained by substituting a_i 's in (3.4).

4. ALGORITHM

Input: level of resolution M .

Step-1: Set collocation points $t_l = \frac{(l-0.5)}{2M}$, $l = 1, 2, 3 \dots 2M$, $M = 2^J$.

Step-2: Compute Haar wavelets $h_i(t)$ and integral of Haar wavelets $I_n h_i(t)$ from Eqs. (2.1) and (2.2), respectively.

Step-3: Construct the system (3.9) by using Eqs. (3.3-3.7) and collocation points t_l sets in step 1.

Step-4: Apply Newton's method to the system (3.9) for unknowns a_i 's

Step-5: Put a_i 's in Eq. (3.4).

Output: Approximate solution $\omega_h(t_l)$.

5. CONVERGENCE ANALYSIS OF HAAR WAVELET

Lemma 5.1. Assume that $\omega(t)$ be any L^2 -space function with bounded first derivative on $[0, 1)$, then the error norm at J^{th} level satisfies the following inequality

$$(5.1) \quad \|e_j(t)\| \leq \sqrt{\frac{K}{7}} C 2^{-(3)2^{J-1}},$$

where K and C are some real constants.

Proof 5.1. For proof see [25].

6. NUMERICAL EXPERIMENT

To check the applicability and efficiency of our technique we have solved second-order linear and non-linear differential equations, integro differential equation, a third-order, and a fourth-order differential equation of pantograph nature. All computer simulations are carried out in MATLAB R2017a and are reported in Tables and figures.

Example 6.1. Consider the pantograph equation

$$(6.1) \quad \omega''(t) = \frac{3}{4}\omega(t) + \omega\left(\frac{t}{2}\right) + \omega'\left(\frac{t}{2}\right) + \frac{1}{2}\omega''\left(\frac{t}{2}\right) - t^2 - t + 1, \quad t \in [0, 1]$$

$$\omega(0) = 0, \omega'(0) = 0.$$

The exact solution of (6.1) from [15] is $\omega_e = t^2$. The present technique is successfully applied on (6.1) and the result is compared with some existing methods [28, 26, 27, 8, 15]. Wavelet coefficients are calculated using classical Newton's method by choosing appropriate initial guess. We observed that Maximum absolute error is zero for $J = 2, 3, 4, \dots, 9$. Also, it is evident from Table 1 and Table 2 that our method has easy applicability and produced better results. Figure 1 shows that both exact and approximate solutions coincide visually.

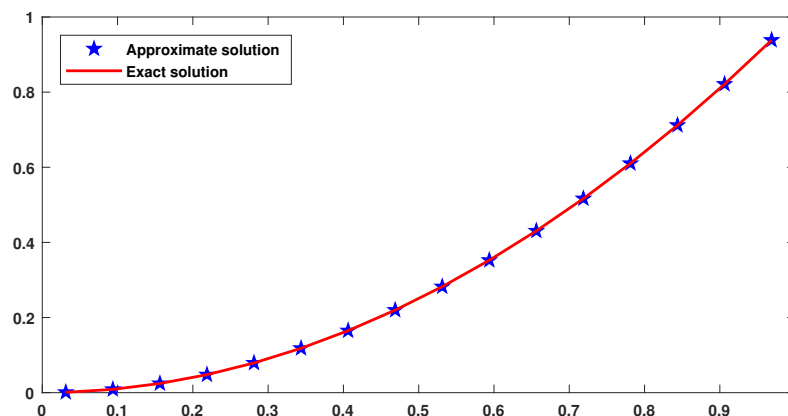


FIGURE 1. Comparison of exact and approximate solution for Example 6.1.

TABLE 1. Error comparison with existing method for Example 6.1.

Our method	Two-stage order-one [28]	One-leg [26] θ-method [27]	VIM[8] $n = 5$	VIM[8] $n = 5$	RKHSM [15] $n = 100$
$J = 2$	RKM	$(\theta = 0.8)$	-	-	-
0	$5.34E - 03$	$2.81E - 01$	$1.11E - 02$	$5.55E - 03$	$4.92E - 04$

TABLE 2. Comparison of exact and approximate solution for Example 6.1.

$t(= 1/32)$	Present method	Exact solution
1.0	0.00097656250	0.00097656250
3.0	0.00878906250	0.00878906250
5.0	0.02441406250	0.02441406250
7.0	0.04785156250	0.04785156250
9.0	0.07910156250	0.07910156250
11.0	0.11816406250	0.11816406250
13.0	0.16503906250	0.16503906250
15.0	0.21972656250	0.21972656250
17.0	0.28222656250	0.28222656250
19.0	0.35253906250	0.35253906250
21.0	0.43066406250	0.43066406250
23.0	0.51660156250	0.51660156250
25.0	0.61035156250	0.61035156250
27.0	0.71191406250	0.71191406250
29.0	0.82128906250	0.82128906250
31.0	0.93847656250	0.93847656250

Example 6.2. In this Example we consider a second order nonlinear pantograph equation

$$(6.2) \quad \omega''(t) = -\omega(t) + \left(\omega\left(\frac{t}{2}\right) \right)^2, \quad t \in [0, 1]$$

$$\omega(0) = 1, \omega'(0) = -2.$$

Approximate solution of (6.2) is obtained with the present algorithm. Our solution is compared with exact solution $\omega_e = \exp(-2t)$ in Table 3 and Figure 2. We have observed that maximum absolute errors are decreased from order of 10^{-3} for $J = 2$ to order of 10^{-7} for $J = 9$.

TABLE 3. Comparison of exact and approximate solution for Example 6.2.

J	$\max y_{exact} - y_{approx} $
3.0	$7.4217E - 04$
4.0	$1.9187E - 04$
5.0	$4.8675E - 05$
6.0	$1.2252E - 05$
7.0	$3.0729E - 06$
8.0	$7.6943E - 07$
9.0	$1.9248E - 07$

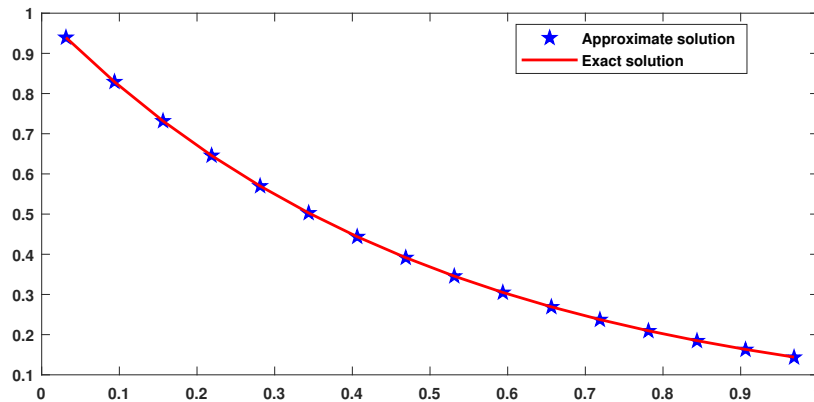
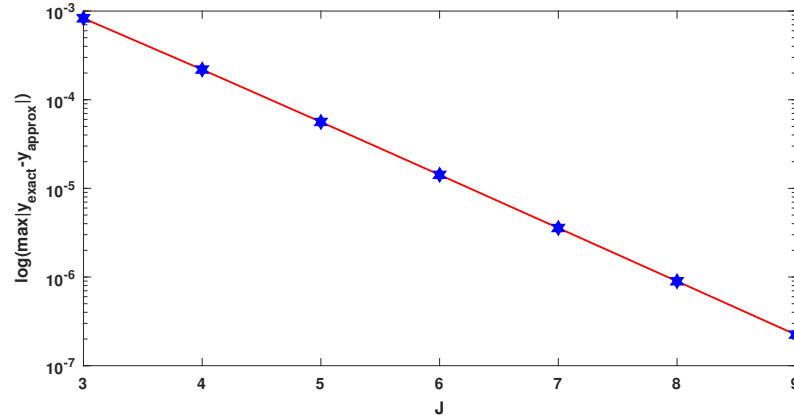


FIGURE 2. Comparison of exact and approximate solution for Example 6.2 at $J = 5$.

Example 6.3. Let us consider the following second order pantograph type initial value problem mention in [15],

$$(6.3) \quad \omega''(t) = \omega' \left(\frac{t}{2} \right) - \frac{t}{2} \omega'' \left(\frac{t}{2} \right) + 2, \quad t \in [0, 1]$$

$$\omega(0) = 1, \quad \omega'(0) = 0.$$

FIGURE 3. Maximum Absolute Errors vs J for Example 6.2.

We have solve this example using present method. The approximate function to be sought is

$$\omega_h = \sum_{i=1}^{2M} a_i * I_3 h_i(t) + t^2 + 1$$

The exact solution of the system (6.3) is $\omega_e = 1 + t^2$. Computer simulation is carried out and it is observed that the maximum absolute error is zero for $J = 2, 3, \dots, 9$. Comparison between approximate solution and exact solution is demonstrated in Figure 4 and Table 4 which shows that both solutions coincide.

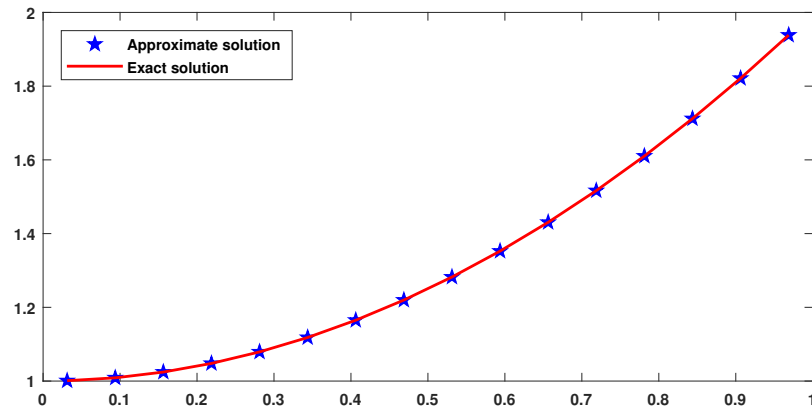


FIGURE 4. Comparison of approximate and exact solution for Example 6.3.

TABLE 4. Comparison of exact and approximate solution for Example 6.3

$t(= 1/16)$	Present method	Exact solution
1.0	1.003906250	1.003906250
3.0	1.035156250	1.035156250
5.0	1.097656250	1.097656250
7.0	1.191406250	1.191406250
9.0	1.316406250	1.316406250
11.0	1.472656250	1.472656250
13.0	1.660156250	1.660156250
15.0	1.878906250	1.878906250

Example 6.4. We consider a nonlinear integro-differential equation with proportional delay in kernal

$$(6.4) \quad \omega'(t) + \left(\frac{t}{2} - 2\right) \omega(t) - 2 \int_0^t \left(\omega\left(\frac{s}{2}\right)\right)^2 ds = 1, \quad t \in [0, 1]$$

$$\omega(0) = 0.$$

Equation (6.4) can be reduced to following second order nonlinear pantograph equation

$$(6.5) \quad \omega''(t) + \left(\frac{t}{2} - 2\right) \omega'(t) + \frac{1}{2} \omega(t) - 2 \left(\omega\left(\frac{t}{2}\right)\right)^2 = 1, \quad t \in [0, 1]$$

$$\omega(0) = 0, \quad \omega'(0) = 1.$$

Now, we have applied present algorithm on (6.5) and obtained its approximate solution. The solution is compared with exact solution $\omega_e = t \exp(t)$ and results are presented in Table 5 and Table 6. We have observed that maximum absolute errors are decreased from order of 10^{-4} for $J = 3$ to order of 10^{-7} for $J = 9$. Also, we have verify in Figure 5 that both solutions visually coincide.

TABLE 5. Comparison of exact and approximate solution for Example 6.4.

J	$\max y_{exact} - y_{approx} $
3.0	$8.2836E - 04$
4.0	$2.1882E - 04$
5.0	$5.6115E - 05$
6.0	$1.4201E - 05$
7.0	$3.5715E - 06$
8.0	$8.9555E - 07$
9.0	$2.2414E - 07$

TABLE 6. Comparison of exact and approximate solution for Example 6.4.

$t(= 1/32)$	Present method	Exact solution	$ y_{exact} - y_{approx} $
1.0	0.0322421468	0.0322419814	$0.1653E - 6$
3.0	0.1029618079	0.1029642319	$0.2423E - 5$
5.0	0.1826661951	0.1826747572	$0.8562E - 5$
7.0	0.2722202080	0.2722387735	$0.1856E - 4$
9.0	0.3725622277	0.3725957133	$0.3348E - 4$
11.0	0.4847113430	0.4847651995	$0.5385E - 4$
13.0	0.6097726143	0.6098534812	$0.8086E - 4$
15.0	0.7489450753	0.7490603671	$0.1152E - 3$
17.0	0.9035281845	0.9036866916	$0.1585E - 3$
19.0	1.0749307939	1.0751423553	$0.2115E - 3$
21.0	1.2646789302	1.2649549829	$0.2760E - 3$
23.0	1.4744259044	1.4747792434	$0.3533E - 3$
25.0	1.7059615777	1.7064068834	$0.4453E - 3$
27.0	1.9612238562	1.9617775258	$0.5536E - 3$
29.0	2.2423096473	2.2429902915	$0.6806E - 3$
31.0	2.5514879480	2.5523163047	$0.8283E - 3$

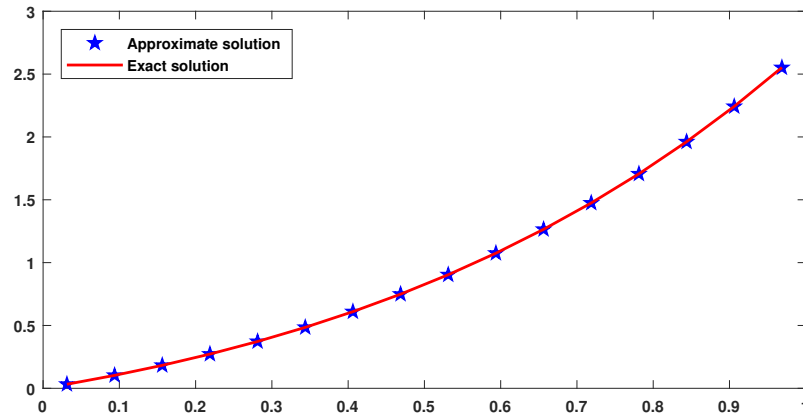


FIGURE 5. Comparison of exact and approximate solution for Example 6.4 at $J = 3$.

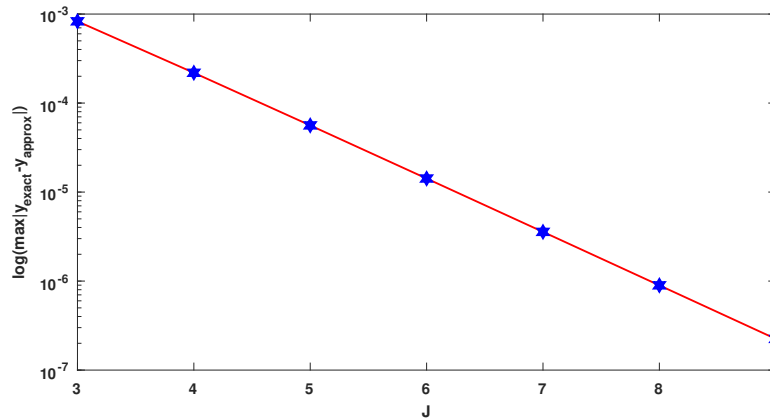


FIGURE 6. Maximum Absolute Errors vs J for Example 6.4.

Example 6.5. In this Example we consider a third-order pantograph equation

$$(6.6) \quad \omega'''(t) = \omega(t) + \omega'\left(\frac{t}{2}\right) + \omega''\left(\frac{t}{3}\right) + \frac{1}{2}\omega'''\left(\frac{t}{4}\right) - t^4 - \frac{t^3}{2} - \frac{4}{3}t^2 + 21t, t \in [0, 1]$$

$$\omega(0) = \omega'(0) = \omega''(0) = 0.$$

We have applied the present algorithm on (6.6). A comparison between approximate and exact solution $\omega_e = t^4$ demonstrated in Figure 7 and it shows that both solutions visually coincide. The wavelet coefficients are calculated using classical Newton’s method with appropriate initial guess. Also, we observed that maximum absolute error for $J = 2$ is of order 10^{-10} . From Tables 7 , 8 , 9 we conclude that present method is more efficient and produced much better result.

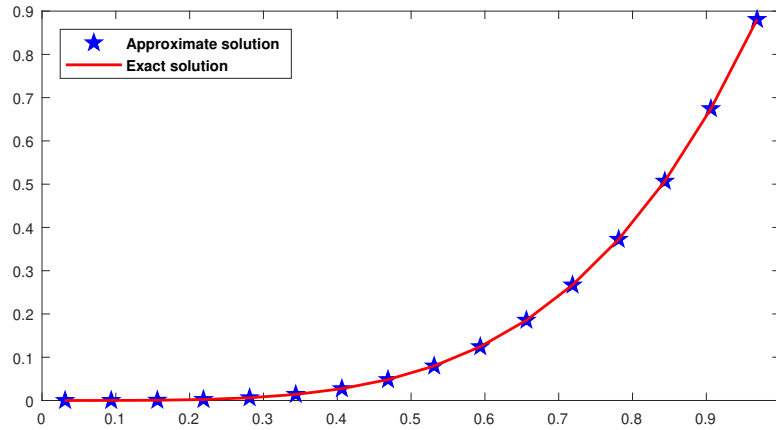


FIGURE 7. Comparison of exact and approximate solution for Example 6.5 at $J = 3$.

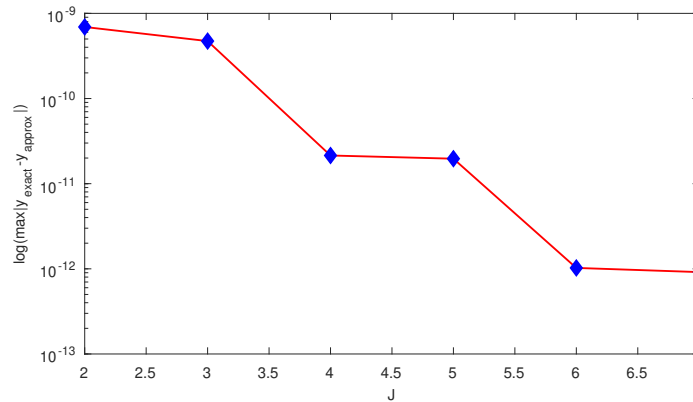


FIGURE 8. Maximum Absolute Errors vs J for Example 6.5.

TABLE 7. Comparison of exact and approximate solution for Example 6.5.

J	$\max y_{exact} - y_{approx} $
2.0	$6.9221E - 10$
3.0	$4.7252E - 10$
4.0	$2.1423E - 11$
5.0	$1.9649E - 11$
6.0	$1.0246E - 12$
7.0	$9.1538E - 13$

TABLE 8. Error comparison with existing method for Example 6.5.

Our method	Two-stage[28]	VIM[8]	VIM[8]	VIM[8]
$J = 2$	order-one RKM	$n = 4$	$n = 5$	$n = 6$
$6.92214E - 10$	$7.34E - 02$	$3.21E - 04$	$4.01E - 05$	$1.26E - 06$

TABLE 9. Comparison of exact and approximate solution for Example 6.5.

$t(= \frac{1}{16})$	Present method	Exact solution	$ y_{exact} - y_{approx} $
1.0	0.000015258789160	0.000015258789063	$0.00098E - 10$
3.0	0.001235961921205	0.001235961914063	$0.07143E - 10$
5.0	0.009536743166434	0.009536743164063	$0.02372E - 10$
7.0	0.036636352518005	0.036636352539063	$0.21057E - 10$
9.0	0.100112915165484	0.100112915039063	$1.26421E - 10$
11.0	0.223403930795185	0.223403930664063	$1.31123E - 10$
13.0	0.435806274199234	0.435806274414063	$2.14829E - 10$
15.0	0.772476195596849	0.772476196289063	$6.92214E - 10$

Example 6.6. Now we consider a fourth order nonlinear multi-pantograph equation

$$(6.7) \quad \omega^{iv}(t) = \omega''\left(\frac{t}{2}\right) \left(\omega^{iv}\left(\frac{t}{4}\right) - \omega(t) \right) + \lambda(t), \quad t \in [0, 1]$$

$$\omega(0) = 0, \quad \omega'(0) = 1, \quad \omega''(0) = 2, \quad \omega'''(0) = 2,$$

where $\lambda(t)$ is given such that system posses the exact solution $\omega_e = e^{(t)} \sin(t)$. Carrying out the numerical technique mention in section 3 we have obtained the approximate solution of (6.7) for different values of J . Maximum absolute errors are computed at different resolution 10. Moreover, the exact solution and approximate solution is plotted in figure 9 for $J = 4$. Based on obtain result, it is realized that the method is efficient to tackle such problems.

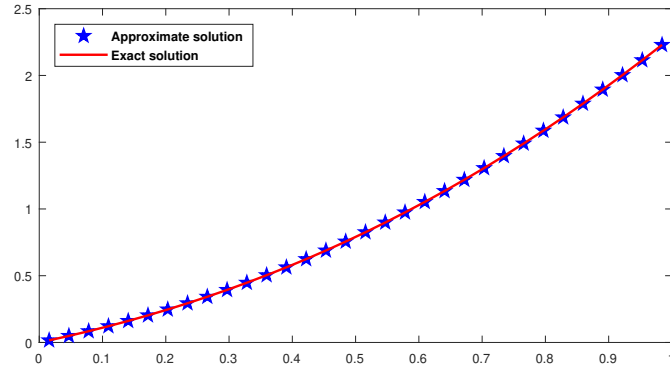


FIGURE 9. Comparison of exact and approximate solution for Example 6.6 at $J = 4$.

TABLE 10. Comparison of exact and approximate solution for Example 6.6 .

J	$\max y_{exact} - y_{approx} $
3.0	$1.6344E - 04$
4.0	$4.3588E - 05$
5.0	$1.9020E - 05$
6.0	$4.8286E - 06$
7.0	$2.2318E - 06$
8.0	$5.5998E - 07$
9.0	$2.6855E - 07$

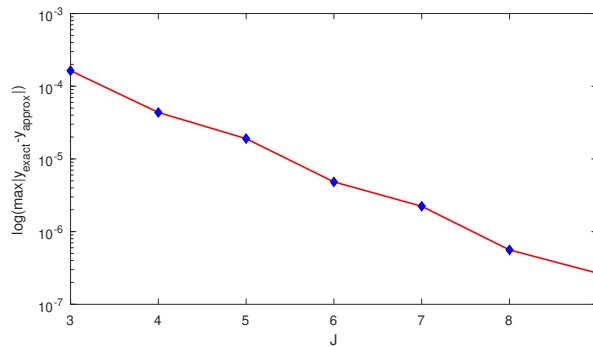


FIGURE 10. Maximum Absolute Errors vs J for Example 6.6.

7. CONCLUSION

A numerical method based on Haar wavelets has been developed for solving a class of delay differential equations known as the pantograph equation. The main advantage of the proposed method is that it transforms the systems of multi-pantograph equations into a system of algebraic equations. Numerical simulations carried out in MATLAB are presented in tables and figures. Comparison with some existing method given in Table 1 and Table 9 shows that the applied method produced better results. Moreover, results presented in Tables 2, 5, 7, and 10 shows that the error reduced with the increase in level of resolution(J). Hence, it is realized that the method is computationally attractive, simple, and is suitable to tackle multi-pantograph equations.

Acknowledgement

The authors are thankful to the editor and reviewers for their valuable suggestions towards the improvement of the paper.

REFERENCES

- [1] A. Abdullah, M. Rafiq, A new numerical scheme based on haar wavelets for the numerical solution of the chen-lee-liu equation, *Optik*, **226** (2021), 165847.
- [2] K. Ahmad, Abdullah, Wavelet Packets and Their Statistical Applications, *Springer*, 2018.
- [3] I. Aziz, R. Amin, Numerical solution of a class of delay differential and delay partial differential equations via haar wavelet, *Appl. Math. Model.*, **40** (2016), 10286–10299.
- [4] M.M. Bahşi, M.Çevik, Numerical solution of pantograph-type delay differential equations using perturbation-iteration algorithms, *J. Appl. Math.*, **2015** (2015), 139821.
- [5] M. Buhmann, A. Iserles, Stability of the discretized pantograph differential equation, *Math. Comput.*, **60** (1993), 575–589.
- [6] M. Cakir, D. Arslan, The adomian decomposition method and the differential transform method for numerical solution of multi-pantograph delay differential equations, *Appl. Math.*, **6(8)** (2015), 1332–1343.
- [7] C.F. Chen, C.H. Hsiao, Haar wavelet method for solving lumped and distributed-parameter systems, *IEE Proceedings-Control Theory and Applications*, **144(1)** (1997), 87–94.
- [8] X. Chen, L. Wang, The variational iteration method for solving a neutral functional-differential equation with proportional delays, *Comput. Math. Appl.*, **59(8)** (2010), 2696–2702.
- [9] R.D. Driver, Ordinary and Delay Differential Equations, *Springer* 1977.

- [10] L. Fox, D.F. Mayers, J.R. Ockendon, A.B. Tayler, On a functional differential equation, *IMA J. Appl. Math.*, **8(3)** (1971), 271–307.
- [11] G. Hariharan, Solving finite length beam equation by the haar wavelet method, *Int. J. Comput. Appl.*, **9(1)** (2010), 0975–8887.
- [12] F. Karakoç, H. Bereketoğlu, Solutions of delay differential equations by using differential transform method, *Int. J. Comput. Math.*, **86(5)** (2009), 914–923.
- [13] U. Lepik, H. Hein, Haar Wavelets: With Applications, *Springer* 2014.
- [14] D. Lu, C. Yuan, R. Mehdi, S. Jabeen, A. Rashid, Approximate solution of multi-pantograph equations with variable coefficients via collocation method based on hermite polynomials, *Commun. Math. Appl.*, **9(4)** (2018), 601–614.
- [15] X. Lv, Y. Gao, The rkhs for solving neutral functional-differential equations with proportional delays, *Math. Meth. Appl. Sci.*, **36(6)** (2013), 642–649.
- [16] J. Majak, B. Shvartsman, K. Karjust, M. Mikola, A. Haavajõe, M. Pohlak, On the accuracy of the haar wavelet discretization method, *Comp. Part B: Eng.*, **80** (2015), 321–327.
- [17] J. Majak, B.S. Shvartsman, M. Kirs, M. Pohlak, H. Herranen, Convergence theorem for the haar wavelet based discretization method, *Compos. Struct.*, **126** (2015), 227–232.
- [18] H.R. Marzban, M. Razzaghi, Rationalized haar approach for nonlinear constrained optimal control problems, *Appl. Math. Model.*, **34(1)** (2010), 174–183.
- [19] J.R. Ockendon, A.B. Tayler, The dynamics of a current collection system for an electric locomotive, *Proc. Roy. Soc. Lond. A.*, **322** (1971), 447–468.
- [20] A. Patra, S. Saha Ray, Numerical simulation based on haar wavelet operational method to solve neutron point kinetics equation involving sinusoidal and pulse reactivity, *Annals of Nuclear Energy*, **73** (2014), 408–412.
- [21] A. Raza, A. Khan, P. Sharma, K. Ahmad, Solution of singularly perturbed differential difference equations and convection delayed dominated diffusion equations using haar wavelet, *Math. Sci.*, (2020), 1–14.
- [22] F.A. Shah, R. Abass, L. Debnath, Numerical Solution of Fractional Differential Equations Using Haar Wavelet Operational Matrix Method, *Int. J. Appl. Comput. Math.*, **3** (2017), 2423–2445.
- [23] H. Song, Y. Xiao, M. Chen, Collocation methods for third-kind volterra integral equations with proportional delays, *Appl. Math. Comput.*, **388** (2020), 125509.
- [24] E. Tohidi, A.H. Bhrawy, K. Erfani, A collocation method based on bernoulli operational matrix for numerical solution of generalized pantograph equation, *Appl. Math. Model.*, **37(6)** (2013), 4283–4294.
- [25] S. Islam, I. Aziz, B. Šarler, The numerical solution of second-order boundary-value problems by collocation method with the haar wavelets, *Math. Comput. Modelling*, **52(9-10)** (2010), 1577–1590.

- [26] W.S. Wang, Shou-Fu Li, On the one-leg θ -methods for solving nonlinear neutral functional differential equations, *Appl. Math. Comput.*, **193(1)** (2007), 285–301.
- [27] W. Wang, T. Qin, S. Li, Stability of one-leg θ -methods for nonlinear neutral differential equations with proportional delay, *Appl. Math. Comput.*, **213(1)** (2009), 177–183.
- [28] W. Wang, Y. Zhang, S. Li, Stability of continuous runge-kutta-type methods for nonlinear neutral delay-differential equations, *Appl. Math. Model.*, **33(8)** (2009), 3319–3329.
- [29] C. Yang, Modified chebyshev collocation method for pantograph-type differential equations, *Appl. Numer. Math.*, **134** (2018), 132–144.

(1) DEPARTMENT OF MATHEMATICS, MAULANA AZAD NATIONAL URDU UNIVERSITY, HYDERABAD, INDIA

Email address: `afroz.ahmad@manuu.edu.in`

(2) DEPARTMENT OF MATHEMATICS, MAULANA AZAD NATIONAL URDU UNIVERSITY, HYDERABAD, INDIA

Email address: `basharathussain_rs@manuu.edu.in`

(3) DEPARTMENT OF MATHEMATICS, ZAKIR HUSSAIN DELHI COLLEGE, UNIVERSITY OF DELHI, INDIA

Email address: `abd.zhc.du@gmail.com`